Proceedings of the Indian National Science Academy (2026) 92:713–725
https://doi.org/10.1007/s43538-025-00447-6

REVIEW ARTICLE

Advances in understanding the Central Indian Tectonic Zone (CITZ): a review of geochemical and geochronological evidences from granite-gneiss and granitoids

Kamaal Parvez[1,2] · M. E. A. Mondal[1] · Iftikhar Ahmad[1] · Wamiq Mohammed Khan[1]

Received: 2 February 2025 / Accepted: 29 April 2025 / Published online: 13 May 2025
© Indian National Science Academy 2025

Abstract
The aim of this study is to provide a comprehensive review of the past decade's published work on geochronological and geochemical attributes of the granite-gneiss and granitoids present in the Central Indian Tectonic Zone (CITZ). This investigation seeks to synthesize recent advancements in the field, providing a cohesive understanding of the geological process involved during the genesis of the studied rocks. In this study, we collate the recent findings and propose that the I-type, H-type and A-type granite-gneiss and granitoid plutons occurring in the CITZ are predominantly derived from the partial melting of the lower continental crust (same source) and linked their emplacement with the dispersal of the Columbia supercontinent.

Keywords Granitoid · Granite-gneiss · Columbia supercontinent · Central Indian Tectonic Zone

Introduction

The Central Indian Tectonic Zone (CITZ) is a key tectonic domain delineating the suture formed due to the amalgamation of the North Indian Block (NIB; includes Bundelkhand and Aravalli cratons) and the South Indian Block (SIB; includes Dharwar, Singhbhum and Bastar cratons) during the Proterozoic Eon (Acharyya 2003). The evolutionary history of the CITZ is very complex and still debated. Numerous models have been put forth thus far to articulate the evolution of the CITZ. Out of them four models of the evolution of the CITZ have been most popular: (i) Early Collision Model: The CITZ is formed by the collision of the NIB and SIB at around ~2.5 Ga and the Central Indian Suture (CIS) marks the line of the collision. The tectonothermal event occurred at around 1.6 Ga and 1.0 Ga (Stein et al. 2004). This model is poorly supported by robust geochronological evidence because of the significant temporal gap between the proposed collision and subsequent tectonothermal events (1.6 and 1.0 Ga), making it difficult to establish a direct genetic linkage and suggesting possible overprinting of older events (Bhowmik 2019). (ii) Sequential Amalgamation Model: The amalgamation of NIB and SIB took place at around 2.2 Ga followed by the two tectonothermal events viz. 1.5 Ga and 0.95 Ga (Mohanty 2023). This model lacks consistent isotopic evidence across the entire CITZ and does not explain complex structural reworking and continuous deformation patterns (Chattopadhyay et al. 2020). (iii) Rodinia Assembly Model: The amalgamation of NIB and SIB is associated with the accretion of the Rodinia supercontinent and took place at around 1.03 Ga to 0.93 Ga (Bhattacharya et al. 2023). This model neglects earlier accretionary events (1.8–1.6 Ga) and oversimplifies the evolution as a single late-stage event (Parvez et al. 2024b). (iv) Multi-Stage Evolution Model: Multi-stage evolution of the CITZ suggests that around 1.8–1.6 Ga CITZ marks an accretionary orogeny (Bhowmik 2019; Chattopadhyay et al. 2020; Parvez et al. 2024a, 2024b). Later, around 1.04–0.94 Ga CITZ marked a continental collision and formed the present form of Indian Landmass (Bhowmik 2019; Chattopadhyay et al. 2020; Bhowmik et al. 2012). The researchers widely accept this model. However, many issues are still unresolved, and face difficulty in unanimously accepting this model because

✉ M. E. A. Mondal
meamondal.gl@amu.ac.in

Kamaal Parvez
kparvez@myamu.ac.in

[1] Department of Geology, Aligarh Muslim University, Aligarh 202002, India

[2] Present Address: Solid Earth Research Group, National Centre for Earth Science Studies, Thiruvananthapuram 695011, India

distinguishing discrete events from overprinted metamorphic signatures, leaving room for debate regarding the exact timing and tectonic nature of each phase.

The subduction polarity of the NIB and SIB is also very perplexing. Yedekar et al., (1990) proposed that NIB subducted beneath the SIB. Later, this model was contradicted by several authors and proposed that SIB subducted beneath NIB (Parvez et al. 2024b, 2024a; Sharma et al. 2022; Roy and Prasad 2003; Wani and Mondal 2016; Giri et al. 2021). Based on seismic reflection profile, Mandal et al., (2013) proposed two northward subductions. However, this model was discarded due to a mismatch between geochemical and geochronological data. Now, the northward subduction model i.e. SIB subducted beneath the NIB is widely accepted (Parvez et al. 2024a, 2024b; Giri et al. 2021; Sharma et al. 2022) (Fig. 1).

The CITZ hosts numerous small granite and granite-gneiss plutons having ages from the late Paleoproterozoic to the early Mesoproterozoic Era. In the northern region of the CITZ, Dudhi granite gneiss (~ 1.75–1.71 Ga; (Shukla et al. 2025), Sidhi granite gneiss (~ 1.72 Ga; Parvez et al. 2024b), Madanmahal granitoid (~ 1.8–1.7 Ga; Parvez et al. 2024b; Yadav et al. 2020), Jhirgadandi granitoid (~ 1.75; Bora et al. 2013), Nerueadamer granitoid (~ 1.88 Ga; Bora 2015), Tumiya granitoid (~ 1.78 Ga; Bora 2015), Katoli granitoid (~ 1.72 Ga; Bora and Kumar 2015), Raspahri granitoid, Harnakachar granitoid (~ 1.72 Ga; Bora 2015) and Sidhi granitoid (~ 1.8–1.6 Ga; Yadav et al. 2020) are exposed whereas Tirodi gneisses (~ 1.7–1.5 Ga; Mishra et al. 2024; Bhowmik et al. 2011) are exposed in the central part of the CITZ. The geochemical characteristics, isotopic signatures, and geochronological data of these granite and granite gneiss served as good proxies for unravelling the complex petrogenetic process and evolution of the CITZ. Several studies have been conducted on these granite gneisses and granitoids in isolation. However, such a large number of plutons were emplaced in a very short duration (~ 0.2 Ga), which raises the question of whether they are derived from the same source and emplaced in similar geodynamic settings or underwent different processes. In this study, we have considered only recently published (past decade) high-quality geochemical data and zircon U–Pb geochronology data. Other dating techniques, such as Rb–Sr and Sm–Nd ages, have not been considered in this study due to a lack of confidence in them in metamorphosed and deformed terranes. In this study, we attempt to structure and collate the recent findings to enhance our understanding of the CITZ evolution and to understand the source of the gneisses and granitoids, whether they are derived from the same source or different sources (Fig. 2).

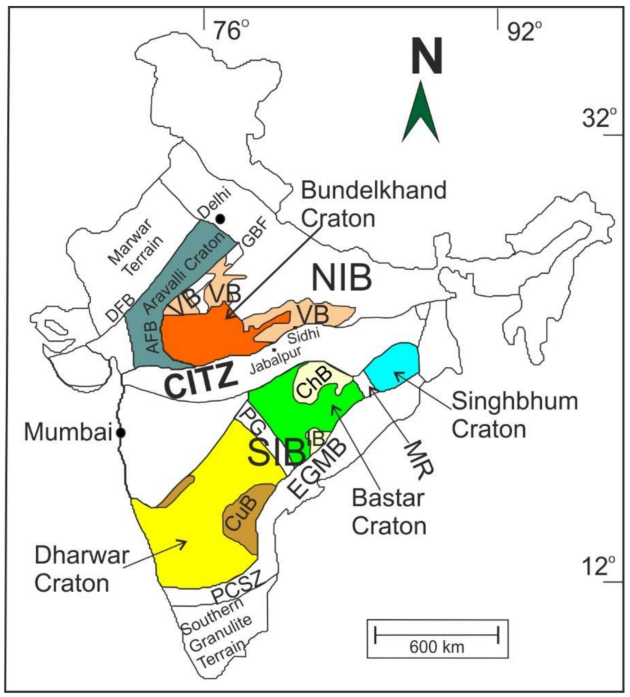


Fig. 1 Outline sketch map of India showing CITZ (Meert and Pandit 2015). *ChB* Chhattisgarh Basin; *CITZ* Central Indian Tectonic Zone; *EGMB* Eastern Ghat Mobile Belt; *GBF* Great Boundary Fault; *PCSZ* Palghat-Cauvery Shear Zone; *MR* Mahanadi Rift; *IB* Indravati Basin; *SIB* South Indian Block; *NIB* North Indian Block; *PG* Pranhita–Godavari Basin; *VB* Vindhyan Basin; *CuB* Cuddapah Basin; *AFB* Aravalli Fold Belt; *DFB* Delhi Fold Belt

Central Indian Tectonic Zone (CITZ): a brief introduction of key Proterozoic suture zone

The CITZ represents a prominent suture zone resulting due to the convergence of the NIB, and the SIB, trending E-W to ENE-WSW (Radhakrishna and Naqvi 1986). The CITZ experienced a protracted tectonothermal evolution between ~ 2.2–0.9 Ga, approximately 1.3 Ga span, marking the amalgamation and assembly of the Columbia (~ 2.1–1.8 Ga) and Rodinia (~ 1.2–0.9 Ga) supercontinents (Rogers and Santosh 2003; Bhowmik et al. 2024; Acharyya and Roy 2000). The CITZ is bounded by the North Son-Narmada Fault (NSNF) at the northern margin and the CIS zone at the southern margin, approximately 200 km in width, consisting of three supracrustal basins viz., Sausar, Betul, and Mahakoshal basins from south to north, respectively. The CITZ consists of various tectonic lineaments along the E-W direction, such as the CIS, Gavilgarh-Tan Shear Zone (GTSZ), South Son-Narmada Fault (SSNF) and NSNF from south to north, respectively (Acharyya and Roy 2000; Roy and Prasad 2003; Acharyya 2003). The Mahakoshal Basin is bounded by the NSNF and SSNF and is situated in the northernmost region of the CITZ. The Mahakoshal Basin is the oldest Paleoproterozoic basin and masks the early evolutionary history of the CITZ. The Betul Basin lies

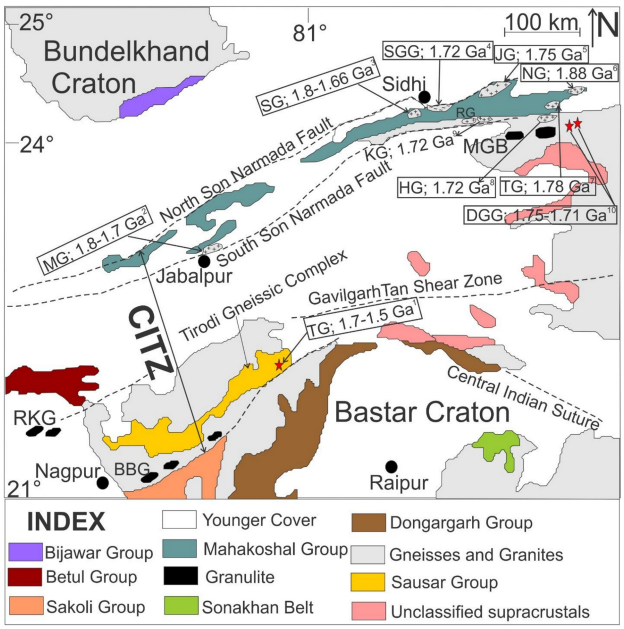


Fig. 2 Map showing different litho-tectonic components of the CITZ (Acharyya and Roy 2000). *CITZ* Central Indian Tectonic Zone; *MGB* Makrohar Granulite Belt; *RKG* Ramakona-Katangi Granulite Belt; *BBG* Balaghat-Bhandara Granulite Belt; *MG* Madanmahal Granitoid; *SG* Sidhi Granitoid; *SGG* Sidhi Granite Gneiss; *JG* Jhirgadandi Granitoid; *NG* Nerueadamer Granitoid; *TG* Tumiya Granitoid; *HG* Harnakachar Granitoid; *KG* Katoli Granitoid; *RG* Raspahari Granitoid; *DGG* Dudhi Granite Gneiss; *TG* Tirodi Gneiss. Age data sources—1: Bhowmik et al. 2011; Mishra et al. 2024; 2: Parvez et al. 2024b; Yadav et al. 2020; 3: Yadav et al. 2020; 4: Parvez et al. 2024b; 5: Bora 2015; Bora et al. 2013; 6: Bora 2015; 7: Bora 2015; 8: Bora 2015; 9: Bora 2015; 10: Shukla et al. 2025

between the SSNF and GTSZ in the middle region of the CITZ and evolved during the Mesoproterozoic Era. The Sausar Basin lies between the GTSZ and CIS at the southernmost margin of the CITZ is the youngest basin of the CITZ. The CITZ encompasses three distinct granulite belts viz. Balaghat-Bhandara granulite, Ramakona-Katangi granulite and Makrohar granulite (Chakrabarty et al. 2022; Chattopadhyay et al. 2020). The Balaghat-Bhandara granulite belt is aligned along the CIS, also marking the southernmost boundary of the CITZ and the Ramakona-Katangi granulite belt is exposed north of the Sausar Basin (Alam et al. 2017; Chattopadhyay et al. 2020). The Makrohar granulite belt is situated south of the Mahakoshal Basin and is sandwiched between SSNF and GTSZ (Chakrabarty et al. 2022). Several granite gneiss plutons are exposed in the CITZ region such as Dudhi granite gneiss, Sidhi granite gneiss and Tirodi gneiss and several small granitoids plutons are also exposed in the CITZ which are named based on the locality in which they are exposed such as Harnakachar granitoid, Jhirgadandi granitoid, Tumiya granitoid, Katoli granitoid, Sidhi granitoid, Nerueadamer granitoid, Raspahri granitoid and Madanmahal granitoid (Bora et al. 2013; Parvez et al. 2024b; Yadav et al. 2020; Bora and Kumar 2015; Table 1). The generalized characteristics of I-type and A-type granites are given in Table 2.

Table 1 Summary of emplacement ages and their respective dating techniques of granite-gneiss and granitoids of the CITZ

S. No	Litho-units	Dating technique	Method	Age (Ga)	References
	Dudhi granite gneiss	zircon U–Pb	LA-ICP-MS	~1.75–1.71	Shukla et al. (2025)
	Sidhi granite gneiss	zircon U–Pb	LA-ICP-MS	~1.72	Parvez et al. (2024b)
	Tirodi gneiss	zircon U–Pb	ID-TIMS	~1.7–1.5	Mishra et al. (2024); Bhowmik et al. (2011)
		Rb–Sr isochron	Whole rock isochron ages	~1.5	Sarkar et al. (1986)
	Katoli granitoid	zircon U–Pb	SHRIMP	~1.72	Bora (2015)
	Nerueadamer granitoid	zircon U–Pb	SHRIMP	~1.88	Bora (2015)
	Tumiya granitoid	zircon U–Pb	SHRIMP	~1.78	Bora (2015)
	Harnakachar granitoid	zircon U–Pb	SHRIMP	~1.72	Bora (2015)
	Jhirgadandi granitoid	zircon U–Pb	SHRIMP	~1.75	Bora et al. (2013)
		Rb–Sr isochron	Whole rock isochron ages	~1.8	Sarkar et al. (1998)
	Sidhi granitoid	zircon U–Pb	ID-TIMS	~1.8–1.66	Yadav et al. (2020)
	Madanmahal granitoid	zircon U–Pb	LA-ICP-MS	~1.8–1.7	Parvez et al. (2024b); Yadav et al. (2020)

Table 2 Generalized characteristics of I-type and A-type granitoids

	I-type granite	A-type granite
Protolith	Igneous	Anhydrous lower crust
Covariate trend	Linear to nearly linear	Linear to nearly linear
A/CNK	< 1.1	< 1.0
CIPW norms	Diopside or < 1% Corundum	Alkalimetasilicate or acmite
SiO_2	53–76%	> 74%
$(^{87}Sr/^{86}Sr)i$	< 0.705	variable
$\delta^{18}O$	< 9‰	variable
K_2O/Na_2O	Low	Na_2O high
Cr, Ni	Low	Low
Fe^{3+}/Fe^{2+}	Moderate	Variable
Large Ion Lithophile Elements (LILE)	High	Low
High Field Strength Elements (HFSE)	Low	High
Petrogenesis/ Geodynamic setting	Melting of infra-crustal mafic to intermediate rocks, subduction zone	Melting of anhydrous lower crust, mantle, fractionation of mafic melt, anorogenic, stable craton, rift zone, hotspot, Post-orogenic rifting

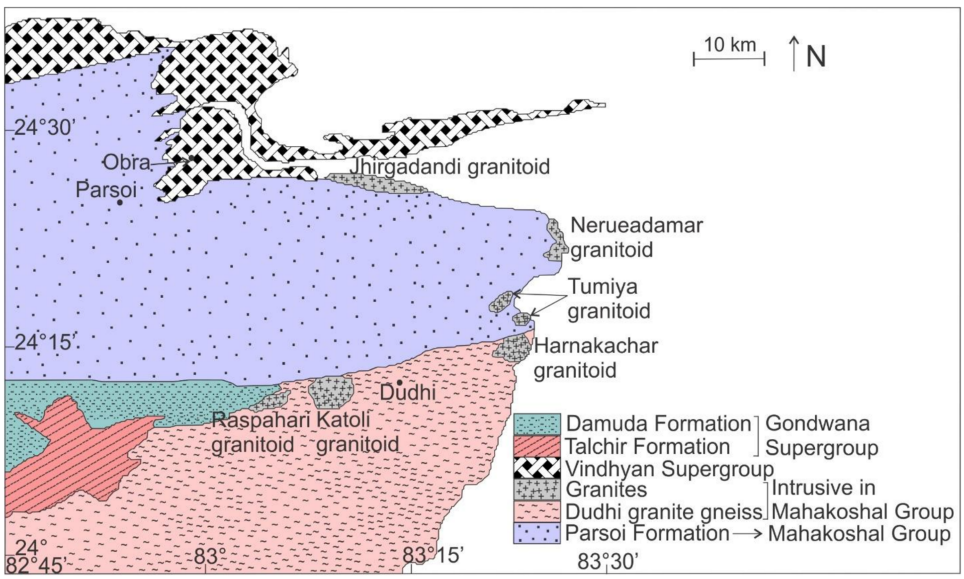


Fig. 3 Geological map showing Jhirgadandi granitoid, Katoli granitoid, Nerueadamer granitoid, Tumiya granitoid, Raspahri granitoid, Harnakachar granitoid, and Dudhi granite gneiss exposed in the eastern part of the CITZ near Dudhi (Raju and Rastogi 2001)

Field relationships of granite-gneiss and granitoid plutons

Dudhi granite gneiss

The granite gneiss is exposed in the Dudhi region, known as the Dudhi granite gneiss (Fig. 3). These rocks are moderately deformed and show folded structures of melanosomes and leucosomes. A fault is passing through the Dudhi granite gneiss known as the Sidhi Fault (Nair 1995). Due to the shearing, the leucocratic melt is produced along the shear zone. However, distal from the fault, it is coarse-grained porphyritic and contains K-feldspar phenocryst and microgranular enclaves along a preferred orientation. Intrusions of mafic dykes are also found in the Dudhi granite gneiss, generally along the foliation direction (NE-SW direction). The gradational contact is observed between the Dudhi granite gneiss and Katoli granitoid.

Sidhi granite gneiss

Sidhi granite gneiss is exposed in and around Sidhi town, Madhya Pradesh (Fig. 4). They are intensely deformed and show numerous micro quartz veins are intruded in them

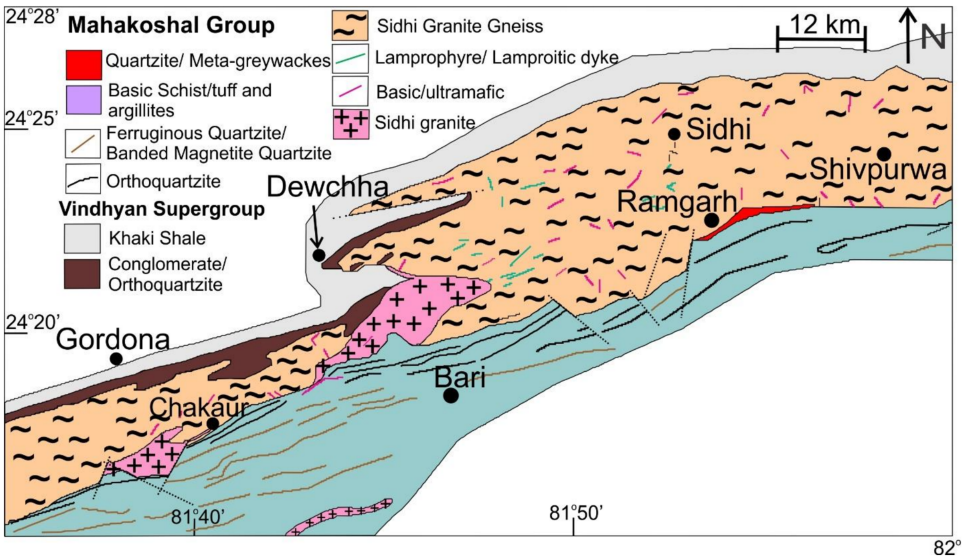


Fig. 4 Geological map showing various litho-units exposed around Sidhi (Narain and Thambi 1977)



Fig. 5 Representative field photograph showing exposure of the Sidhi granite gneiss intruded by the micro-quartz veins trending NE-SW direction near Sidhi

(Fig. 5). These quartz veins are aligned in the E-W direction. The leucosomes and melanosomes bands are distinctly observed. Moreover, Sidhi granite gneiss bears identical field observations with Dudhi granite gneiss, which might be due to the Dudhi granite gneiss being the eastward extension of the Sidhi granite gneiss.

Tirodi gneiss

The Tirodi gneiss, sometimes referred to as Tirodi Biotite Gneiss (TBG), is a biotite-bearing gneiss which is exposed between the GTSZ and CIS (Fig. 2). Tirodi gneiss is intercalated with the amphibolite, meta-pelites, mafic granulites and feldspathic mica schist. The meta-sedimentary rocks and meta-igneous rocks are highly deformed and occur as rafts and enclaves within the Tirodi gneiss. The stratigraphic status of the Tirodi gneiss has been debated among geologists for the past several decades. Initially, Tirodi gneiss was considered the basement of the supracrustals rocks of the Sausar Group (Narayanaswamy et al. 1963). However, subsequent studies made contention and suggested that the Tirodi gneiss are produced due to the anatexis of the basement rocks of the Sausar Group or they are igneous rocks which are intruded in the Sausar Group (Sarkar et al. 1986). Recent studies suggest that Tirodi gneiss is the collage of various litho-units including enclaves of mafic and ultramafic rocks, foliated granites, and orthogneisses (Bhowmik and Roy 2003; Mishra et al. 2024; Bhowmik and Pal 2000).

Katoli and Raspahari granitoids

Katoli granitoids are well exposed in and around Katoli village near Dudhi (Fig. 3). They are coarse to medium grained varying from leucocratic to mesocratic granitoids. These granitoids show an intrusive relationship with the mica schist and carbonates of the Mahakoshal Group. The xenoliths of meta-volcanics and meta-sedimentary rocks are embedded in the host granitoids. The meta-sedimentary (mica schist) xenoliths retain their metamorphic fabric (schistose fabric; Bora 2015). The Katoli granitoid shows a gradational relationship from mesocratic to leucocratic granitoids. Occasionally, mafic dykes and feldspathic veins are intruded in the Katoli granitoids. The feldspathic veins are disengaged along the direction of shearing, suggesting that the syntectonic emplacement of feldspathic veins is due to tectonic activity in the CITZ, which is aligned along the E-W direction.

Raspahari granitoids are well exposed in the southeast region from the Dudhi granite gneiss, adjacent to the Katoli granitoid pluton (Fig. 3). This granitoid pluton is named after the Raspahari area in which they are exposed. They are similar to Katoli granitoid in appearance. Similar to

Katoli granitoid, Raspahari granitoid are coarse to medium grained mesocratic and contain enclaves of meta-argillites of the Mahakoshal Group. The xenoliths of meta-argillites are aligned parallel to the regional foliations.

Nerueadamer and Tumiya granitoids

The two small adjacent granitoid plutons exposed in the eastern part of the CITZ are well-exposed and named after the locality in which they are well-exposed (Fig. 3). However, both the granitoid plutons show similar field observations, such as identical textural and compositional features. Both the granitoids are leucocratic to mesocratic and show an intrusive relationship with the meta-argillites of the middle formation of the Mahakoshal Group (i.e. Parsoi Formation). The xenoliths of meta-argillites are aligned parallel, indicating that the rocks have undergone post-depositional deformation. The presence of xenoliths of the meta-argillites also gives clues about their intrusive nature in the Mahakoshal Group.

Harnakachar and Jhirgadandi granitoids

Harnakachar granitoids are coarse-grained and well-exposed in the Harnakachar area southeast of the Dudhi granite gneiss (Fig. 3). They lack country rock xenoliths, and due to the thick regolith cover around the pluton, it is difficult to identify whether they are intrusive in the Mahakoshal Group or basement rocks. Harnakachar granitoid is intruded by the mafic dykes and aplitic veins.

Jhirgadandi granitoid pluton is situated at the northernmost margin of the CITZ, well-exposed near Jhirgadandi and Pipraha village, Madhya Pradesh (Fig. 3). Compared to other granitoid plutons exposed in and around the Mahakoshal Basin, the Jhirgadandi pluton has vast exposure. The Jhirgadandi granitoids contain xenoliths of country rock (meta-argillites and chert of the Mahakoshal Group) suggesting that they are younger than the Mahakoshal Group. The xenoliths are aligned along the axis of the CITZ i.e. E-W direction. This pluton is medium to coarse-grained, porphyritic granitoid containing an adequate amount of biotite.

Sidhi and Madanmahal granitoids

Sidhi granitoid is exposed in and around Sidhi town in the vicinity of Sidhi granite gneiss (Fig. 4). They are coarse to medium grained mesocratic, varying in colour from pink to grey. They are foliated and near shear zones, showing deformation structures along the E-W direction. Along the southern margin of the pluton, the porphyritic texture is best exposed near Tikari village, Madhya Pradesh. The porphyritic texture is characterized by the large phenocryst of the feldspar. An adequate amount of dark biotite grains can be seen in some places.

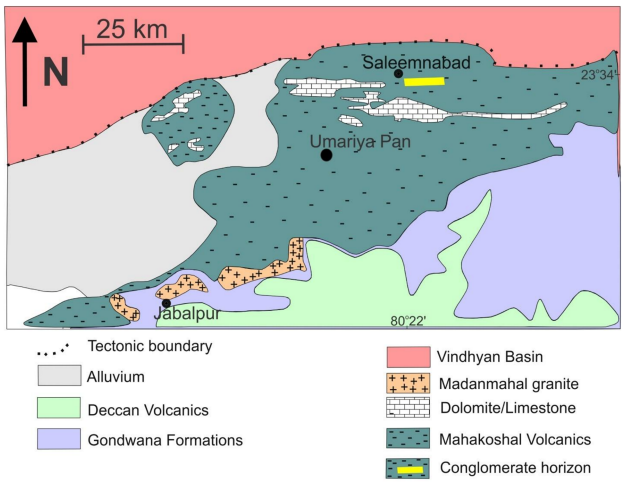


Fig. 6 Geological map showing various litho-units exposed near Jabalpur (Khanna et al. 2017)

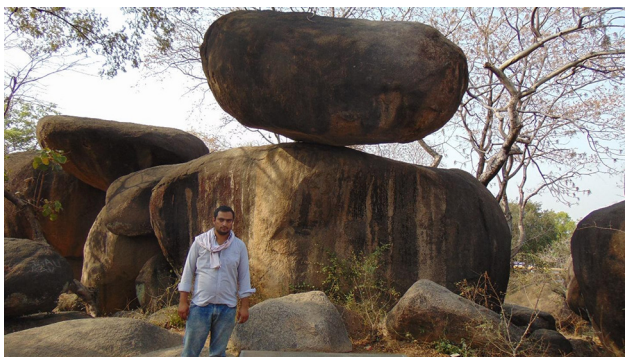


Fig. 7 Representative field photograph showing exposure of the Madanmahal granitoid near Jabalpur

Madanmahal granitoid pluton is exposed in and around Jabalpur, Madhya Pradesh, in the eastern part of the CITZ (Fig. 6). This pluton varies in colour from pink to grey, equigranular, and coarse to medium grained (Fig. 7). However, grain size shows the gradational change from coarse to medium-grained from the core to the periphery of the pluton. This pluton is intruded into the meta-argillites of the Mahakoshal Group, and in some places, they are characterized by weakly developed foliations. The Madanmahal granite is intruded by apalite, pegmatite, and quartz veins.

Geochemical and geochronological constraints

Dudhi granite gneiss

The Dudhi granite gneiss varies in composition from monzonite to granodiorite in the total alkalis silica (TAS) diagram. The rare earth elements (REE) pattern is highly fractionated with negative Eu anomaly. The primitive mantle (PM) normalized multi-element diagram shows Nb, Ba, Ti, and Sr anomalies (Shukla et al. 2025). These rocks are enriched in high-field strength elements (HFSE) and depleted in large ion lithophile elements (LILE) and show metaluminous character (Shukla et al. 2025). The Dudhi granite gneiss shows I-type granite characteristics (Bora and Kumar 2015). The εNd(t) values at t = 1.7 Ga of Dudhi granite gneiss ranges from -5.7 to -0.4 and T_{DM} (Nd; model age) varies from 2.42 to 2.07 Ga (Shukla et al. 2025). The negative values of εNd(t) give clues that the studied rocks are formed due to the partial melting of the older crust. Earlier, Ramakrishnan and Vaidyanadhan, (2008) proposed that the Dudhi granite gneiss and Sidhi granite gneiss served as the basement for the Mahakoshal Group (~ 2.2–1.8 Ga). Recently, Shukla et al., (2025) obtained their crystallization age from zircon U–Pb systematics to be ~ 1.75–1.71 Ga suggesting that the studied granite gneiss pluton is younger than the Mahakoshal Group (Table 1). Deshmukh et al., (2017) obtained monazite U-Th-Pb ages from the Dudhi gneissic complex during ~ 1.7 Ga and determined the clockwise P–T path.

Sidhi granite gneiss

The Sidhi granite gneiss is compositionally categorized as granite in the TAS diagram. They are strongly peraluminous in character, vary from calcic to alkali calcic and ferroan in nature. These rocks show high fractionation in REE patterns with prominent Eu anomaly (Parvez et al. 2024b). The PM normalized multi-element diagram exhibits Ba, Nb, Ti, and Sr anomalies (Parvez et al. 2024b). These studied rocks are also depleted in LILE and enriched in HFSE. They are akin to A-type granite characteristics and are further categorized into A_2-type granite (Parvez et al. 2024b). Parvez et al., (2024b) suggest that the studied rocks are formed due to the partial melting of the Bundelkhand gneiss and granite. The emplacement age of the Sidhi granite gneiss obtained from the zircon U–Pb is ~ 1.72 Ga (Parvez et al. 2024b; Table 1).

Tirodi gneiss

The Tirodi gneiss varies in composition from monzonite to granodiorite in the TAS diagram. They have a calc-alkaline lineage and consist of metaluminous to peraluminous characteristics. The REE patterns of Tirodi gneiss suggest that they are highly fractionated and show negative Eu anomaly (Mishra et al. 2024). The PM normalized multi-element diagram exhibits Ba, Nb, Ti, and Sr anomalies (Mishra et al. 2024). These rocks are categorized as A-type granites which are further subcategorized as A_2-type granites (Mishra et al. 2024). $^{143}Nd/^{144}Nd$ at t = 1.7 Ga varies from 0.509898 to 0.510508 and εNd(t) values ranges from + 0.58 to -10.59 (Mishra et al. 2024). The negative values to slightly positive values suggest that heterogeneous crustal sources. The T_{DM} ages vary from 2.95 to 2.11 Ga (Mishra et al. 2024). The εHf(t) ranges from + 3.7 to -3.3 corroborating the heterogeneous sources and T_{DM} (Hf) from 2.52 to 2.09 Ga (Bhowmik et al. 2011). The zircon U–Pb ages suggest that Tirodi gneiss are emplaced between ~ 1.7 to 1.5 Ga (Bhowmik et al. 2011; Mishra et al. 2024; Table 1). Earlier, Sarkar et al., (1986) obtained whole rock Rb–Sr isochron ages of Tirodi gneiss to be ~ 1.5 Ga (Table 1).

Katoli and Raspahari granitoids

Katoli granitoids belong to a sub-alkaline series varying in composition from monzonite to granite in the TAS diagram. They show tholeiitic to calc-alkaline lineage and exhibit strongly metaluminous in nature. The studied rocks are shown to have high fractionation in REE and exhibit negative Eu anomaly (Bora 2015; Bora and Kumar 2015). The PM normalized multi-element diagram exhibits Ba, Nb, and Ti anomalies (Bora 2015). Katoli granitoids are alkali-calcic to calc-alkalic and exhibit I-type granite characters (Bora and Kumar 2015). The crystallization age of the Katoli granitoids obtained from the zircon U–Pb systematics is ~ 1.72 Ga (Bora and Kumar 2015; Table 1).

Raspahari granitoid shows similar characteristics to Katoli granitoid. Raspahari granitoids vary in composition from monzonite to granite in the TAS diagram. They exhibit calc-alkaline character and show a strongly peraluminous nature. Raspahari granitoids are calc-alkalic to alkali-calcic characteristics and exhibit I-type granite characteristics (Bora and Kumar 2015). The REE patterns of Raspahari granitoids show strong fractionation and large negative Eu anomaly (Bora 2015; Bora and Kumar 2015). The PM normalized multi-element diagram exhibits Ba, Nb, and Ti anomalies (Bora 2015).

Nerueadamer and Tumiya granitoids

Nerueadamer granitoids compositionally belong to granite in the TAS diagram. They are ferroan in nature and belong to the calc-alkaline series. Nerueadamer granitoids exhibit peraluminous character and show I-type granite characteristics (Bora 2015; Bora and Kumar 2015). Nerueadamer granitoids show high fractionation in REE patterns and prominent Eu anomaly (Bora 2015; Bora and Kumar 2015). The PM normalized multi-element diagram exhibits Ba, Nb, and Ti anomalies (Bora 2015). The emplacement age of the Nerueadamer granitoids obtained from the zircon U–Pb systematics is ~ 1.88 Ga (Bora 2015; Table 1).

Tumiya granitoids compositionally belongs to granite in the TAS diagram. They vary in nature from tholeiitic to calc-alkaline series and ferroan to magnesian. Tumiya granitoids are peraluminous, calc-alkalic and exhibit H-type granite characters (Bora 2015; Bora and Kumar 2015). The REE patterns of the studied rocks exhibit that they are highly fractionated with prominent Eu anomaly (Bora 2015; Bora and Kumar 2015). The PM normalized multi-element diagram exhibits Ba, Nb, and Ti anomalies (Bora 2015). The crystallization age of the Tumiya granitoids obtained from the zircon U–Pb systematics is ~ 1.78 Ga (Bora 2015; Table 1).

Harnakachar and Jhirgadandi granitoids

Harnakachar granitoids are categorized into sub-alkaline series and monzodiorite in composition in the TAS diagram (Bora 2015). They are highly magnesian, calc-alkaline and strongly meta-aluminous in nature. The REE patterns of the studied rocks are highly fractionated with strong Eu anomaly (Bora 2015; Bora and Kumar 2015). The PM normalized multi-element diagram exhibits Ba, Nb, and Ti anomalies (Bora 2015). Harnakachar granitoids show H-type granite characteristics (Bora 2015; Bora and Kumar 2015). The crystallization age of the Harnakachar granitoids obtained from the zircon U–Pb systematics is ~ 1.72 Ga (Bora 2015; Table 1).

Jhirgadandi granitoids are categorized into sub-alkaline series and their composition ranges from monzodiorite to granite in the TAS (Bora et al. 2013). They are dominantly metaluminous, calc-alkaline and magnesian in nature (Bora 2015; Bora et al. 2013). The REE patterns of the studied rocks are strongly fractionated and exhibit prominent Eu anomaly (Bora 2015; Bora and Kumar 2015). The PM normalized multi-element diagram exhibits Ba, Nb, and Ti anomalies (Bora 2015). Jhirgadandi granitoids exhibit I-type granite characteristics (Bora et al. 2013). The crystallization age of the Jhirgadandi granitoid pluton obtained from the zircon U–Pb systematics is ~ 1.75 Ga (Bora 2015; Bora et al. 2013; Table 1). Earlier, Sarkar et al., (1998) obtained whole rock Rb–Sr isochron ages yielding ~ 1.81 Ga (Table 1).

Sidhi and Madanmahal granitoids

Sidhi granitoids are compositionally characterized as granite in the TAS diagram. They are ranging from calc-alkalic to alkali-calcic, metaluminous to peraluminous and ferroan in nature (Yadav et al. 2020). They are characterized by enriched REE patterns with negative Eu anomaly and HFSE (Zr and Y) and depleted LILE (Ba and Sr). The studied granites consist of high zircon saturation temperature (ZST) > 900 °C and shows negative anomalies of Sr, Ti and Nb. Sidhi granitoids exhibits A-type granite characteristics which are further sub-categorized into A_2-type granite. The εNd(t) at t = 1.7 Ga ranges from − 9.8 to − 5.6 and T_{DM} varies from 2.96 to 2.48 Ga suggesting the crustal sources contribution during their genesis (Yadav et al. 2020). The zircon U–Pb ages of the Sidhi granite suggest that Sidhi granite is emplaced during ~ 1.8 to 1.66 Ga (Yadav et al. 2020; Table 1).

Madanmahal granitoids are compositionally characterized as granites in the TAS diagram. They are strongly peraluminous, alkali-calcic and ferroan in nature (Parvez et al. 2024b). Further, they exhibit high fractionation in REE patterns with prominent Eu anomaly. Moreover, Madanmahal granitoids show depleted LILE and enriched HFSE with negative Ba, Nb. Sr, and Ti anomalies. ZST of the studied rocks is > 900 °C. The Madanmahal granitoids are akin to A-type granites which are further sub-categorized as A_2-type granites (Parvez et al. 2024b; Yadav et al. 2020). The εNd(t) at t = 1.7 Ga ranges from -11.4 to -8.2, and T_{DM} varies from 3.14 to 2.59 Ga, suggesting that they are derived from the older continental crust (Yadav et al. 2020). The crystallization age of the Madanmahal granitoid pluton obtained from the zircon U–Pb systematics is ~ 1.8–1.7 Ga (Parvez et al. 2024b; Yadav et al. 2020; Table 1).

Discussion

The CITZ contains several small granite-gneiss and granitoid plutons which exhibit similar types of geochemical characteristics and have crystallization ages between ~ 1.8–1.6 Ga. The geochemical studies suggest that Katoli granitoids, Nerueadamer granitoids, Raspahari granitoids, Jhirgadandi granitoids and Dudhi granite gneiss exhibit I-type granite characters, Tumiya granitoids and Harnakachar granitoids exhibit H-type granite characters and Sidhi granite gneiss, Tirodi granite gneiss, Sidhi granitoids and Madanmahal granitoids exhibit A-type granite characteristics. I-type granite is metaluminous in nature, H-type granite is a transitional type that varies from metaluminous to peraluminous in nature, and A-type granite is peraluminous in nature (Bora 2015; Parvez et al. 2024b; Bora et al. 2013; Yadav et al. 2020, 2015; Bora and Kumar 2015; Table 3). However,

Table 3 Summary of geochemical and geochronological parameters of granite gneiss and granitoid plutons exposed in the CITZ

Geochemical Parameters	Dudhi granite gneiss	Sidhi granite gneiss	Tirodi gneisses	Jhirgadandi granitoid	Katoli granitoid	Nerueadamer granitoid	Raspahri granitoid	Tumiya granitoid	Harnakachar granitoid	Madanmahal granitoid	Sidhi granitoid
SiO_2 (wt%)	68.13–72.62	68.95–75.04	65.3–78.1	50.7–72.18	57.52–77.49	68.38–72.53	66.96–72.43	69.27–72.58	51.41–57.12	70.17–72.99	64.47–77.87
A/CNK	0.66–1.05	1.22–3.35	0.72–1.5	0.63–1.05	0.50–1.17	1.19–1.27	1.04–1.15	1.08–1.11	0.91–1.09	1.04–1.35	1.0–1.11
Cr, Ni	Low	Low	Low	Low	Low	Low	Low	Low	Low	Low	Low
LILE (Ba, Rb, Sr)	High	High	High	Moderate	Moderate	Moderate	Moderate	High	High	High	High
HFSE (Zr, Hf, Ti, Nb)	High	High	High	High	High	High	High	High	High	High	High
$(La/Yb)_N$	19.71–80.45	3.27–13.82	1.6–83.5	12.35–44.11	5.29–90.99	5.80–43.21	30.04–182.91	7.16–19.69	7.75–38.29	7.08–17.71	3.68–32.6
Classification	A-type	A-type	A-type	I-type	I-type	I-type	I-Type	H-type	H-type	A-type	A-type
εNd(t)	− 5.7 to − 0.4	NA	− 10.59 to + 0.58	NA	NA	NA	NA	NA	NA	− 11.4 to − 8.2	− 9.8 to − 5.6
Tectonic Interpretation	Post-orogenic setting	Post-orogenic setting	Post-orogenic setting	Syn to post-orogenic setting	Syn to post-orogenic setting	Syn-orogenic setting	Post-orogenic setting	Syn-orogenic setting	Post-orogenic setting	Post-orogenic setting	Post-orogenic setting

$_N$: Chondrite normalized (McDonough and Sun 1995); *NA* - not available

they show similar multi-element diagrams and REE patterns (show negative Nb, Ba, Ti, Sr and Eu anomalies) suggesting that they are derived from the same source. The ε Nd values of Sidhi granitoids and Madanmahal granitoids are overlapping further corroborate that they are derived from the same source (Yadav et al. 2020). The simultaneous occurrence of I-type granite and A-type granite looks contradicting at first glance because the source rocks of both granites are assumed to be different. However, recently several geochemical and Nd isotopic studies have been conducted which argue that I-type granite and A-type granite can be produced from the same source (Huang et al. 2023; Parvez et al. 2024b; Wang et al. 2018). The initial partial melting of the lower crust can produce metaluminous I-type granite melt and later stages of partial melting of the lower crust can produce peraluminous A-type granite melt (Parvez et al. 2024b; Wang et al. 2018). In the Jiuhuashan area in south China, the simultaneous presence of I-type and A-type granites was found (Wang et al. 2018). Similarly, in east Junggaer, NW China concurrent occurrence of A-type and I-type granites are found (Huang et al. 2023).

The most persistent issue among the researchers is how pre-existing rocks accommodate the intrusions of newly incoming magma, which is generally referred to as a space problem. Addressing the space problem is most concerning, especially for the emplacement of the extensive batholithic volumes of magma during the single magmatic episode. Recent advancements have significantly enhanced our understanding of this problem. Tectonic activity plays a crucial role in creating the necessary space within the crust to accommodate large volumes of magma. Recent studies suggest that the emplacement of the magma does not occur in a single magmatic episode but in an episodic magmatic event i.e. discrete magma pulse (Petford et al. 1994, 1993). During the ascending of the magma, hot underplated magma comes in contact with the cold crustal rocks causing changes in the volume of the crustal rocks and leading to local fracturing (Petford et al. 1993, 1994, 2000). This is the probable reason why we get discrete and scanty granitoids in the CITZ. Similar sparse granitoid plutons are also observed in the Aravalli Craton (Ahmad et al. 2023).

Affinity with Columbia supercontinent

The emplacement of I-type and A-type granites during the 1.8–1.6 Ga interval is closely linked to the tectonic processes coupled with the dispersal of the Columbia supercontinent. I-type granites, typically formed in subduction-related orogenic settings, and A-type granites, often associated with extensional tectonic regimes, reflect the evolving tectonic framework during the Paleoproterozoic Era. The coexistence of A-type, H-type and I-type granites, which are also found in south China, in Labrador, Canada and NW China, align

temporally with the transition from convergent to extensional regimes during the Paleoproterozoic Era (Ketchum et al. 2001; Huang et al. 2023; Wang et al. 2018). This transition marks a shift in tectonic forces, possibly driven by the initial stages of the dispersal of the Columbia supercontinent and causes the localized extension (Kaur et al. 2011; Y. Wang et al. 2020a, b). In contrast, I-type granites, typically associated with arc magmatism and subduction processes, highlight ongoing crustal recycling and reworking during this time. Their emplacement underscores the continuation of active tectonic boundaries and magmatic arcs during the gradual dispersal of Columbia (1.8–1.5 Ga).

Furthermore, comparison and correlation of the geochemical and geochronological signatures of the studied granite gneisses and granitoids with coeval Paleoproterozoic granitoids from other continental blocks including Asia (India and China), Africa and Australia, provide valuable insights into global crust-forming processes and continental growth. Geochemical data reveal that the granite gneisses and granitoids of the CITZ share compositional characteristics with these intercontinental granitoids. Additionally, geochronological data highlight significant episodes of granitic magmatism and crust formation during 2.1 to 1.6 Ga on a global scale (Bhowmik et al. 2011; Wang et al. 2020a, b; Huang et al. 2023; Kaur et al. 2011; Kirkland et al. 2011; Li et al. 2019; Kröner et al. 2010; Manya and Maboko 2016; Mishra et al. 2024; Okonkwo and Ganev 2012; Gupta and Kumar 2023; Parvez et al. 2024a; Sheppard et al. 2004; Dwivedi et al. 2023; Zhao et al. 2020; Chen and Xing 2016; Fig. 8).

The tectono-magmatic evolution of the granite gneisses and granitoids of the CITZ, when considered in the context of other global cratonic blocks, offers critical constraints on the geological evolution of the CITZ and its connection to the Columbia supercontinent. Columbia supercontinent is conjectured to have existed during widespread Paleoproterozoic orogenic cycles (2.1–1.8 Ga), uniting continental fragments including Laurentia, North China, Amazonia, India, Australia, and Africa (Meert 2012; Rogers and Santosh 2003). The disintegration of the Columbia supercontinent started ~ 1.8 Ga and is well documented, with its assembly likely initiated between 1.90 and 1.85 Ga, as indicated by widespread intracontinental extensional tectonics and anorogenic magmatism (Rogers and Santosh 2002). The presence of A-type granites is a key marker of such tectonic transitions, often associated with episodes of continental rifting or breakup during supercontinent cycles. This association is particularly evident in the CITZ, where the occurrence of Paleoproterozoic rift-related magmatism indicates a transition from collisional to extensional regimes, supported by widespread anorogenic magmatic activity (Bora 2015; Parvez et al. 2024b; Bora et al. 2013; Yadav et al. 2020). These rifting

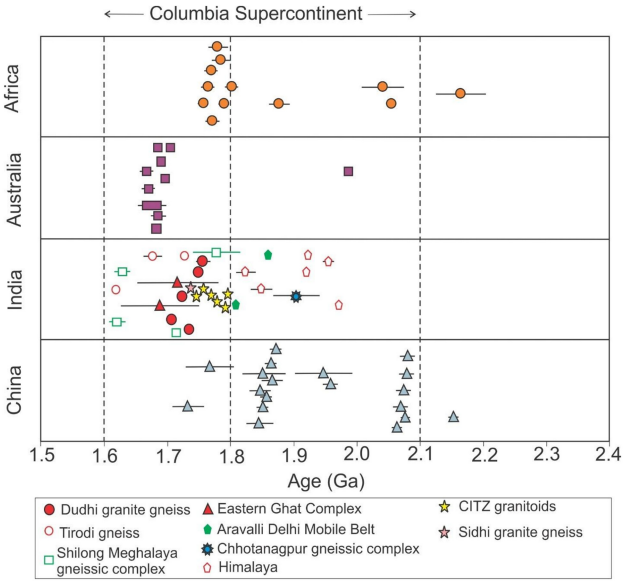


Fig. 8 Distribution of Paleoproterozoic magmatism from different continental blocks globally to understand the evolution of the CITZ compared to other parts of the world and linked their evolution to the Columbia Supercontinent. Ages were taken from the following sources: Africa (Bonzi et al. 2021; Kröner et al. 2010; Manya and Maboko 2016; Okonkwo and Ganev 2012); India (Bora 2015; Bora et al. 2013; Dwivedi et al. 2023; Kaur et al. 2011; Mishra et al. 2024; Parvez et al. 2024b; Shukla et al. 2025; Yadav et al. 2020); China (Chen and Xing 2016; Huang et al. 2023; Li et al. 2019; J. Wang et al. 2020a, b; Zhao et al. 2020); Australia (Kirkland et al. 2011; Sheppard et al. 2004)

phases are closely alligned with the disintegration of the Columbia supercontinent, as corroborated by comparable magmatic events documented in different parts of the world such as China, Africa and Amazonia (Bonzi et al. 2021; Li et al. 2019; Kirkland et al. 2011; Zhao et al. 2003).The polarity of the subduction of NIB and SIB has been under extensive debate among geoscientists. Earlier, a southward subduction model was proposed i.e. NIB subducted beneath the SIB (Yedekar et al. 1990). Later studies contradict the previous studies and suggest a northward subduction model i.e. SIB subducted beneath the NIB (Sharma et al. 2022; Parvez et al. 2024b, 2024a; Wani et al. 2022; Chattopadhyay et al. 2017; Roy and Prasad 2003; Wani and Mondal 2016). The presence of abundant I-type and A-type granitoids in the CITZ suggests that the post-orogenic extensional tectonic setting might be due to the transition from a convergent to a divergent setting.

Conclusions

The CITZ hosts several sparse granite-gneiss and granitoid plutons exhibiting geochemical affinities with I-type, H-type and A-type granitic affinity. The studied granitoids and granite-gneiss show similar geochemical signatures and are emplaced between 1.8 to 1.5 Ga. The geochemical and isotopic signatures of the studied granite-gneiss and granitoids are formed due to the partial melting of the lower continental crust. Several small plutons are emplaced due to the local fracturing, which might be due to dilation changes that occur due to the interaction of hot magma with cold crustal litho-units. Additionally, the tectonic processes linked with the dispersal of the Columbia supercontinent, i.e. transition from subduction-related process to extensional process, appear to have played a significant role in controlling the emplacement dynamics of these studied granite-gneiss and granitoid plutons. Despite the fact that lots of data have been generated in the past decade, CITZ needs more attention to track its evolutionary history. The mineral chemistry of these granitoid plutons can help to explore more to understand their genesis and source of these granitoid and granite gneiss, which provide robust evidence of their petrogenesis.

Acknowledgements We thank the Chairperson, Department of Geology, A.M.U., Aligarh, for extending the necessary facilities during this research work.

Author contributions Kamaal Parvez and M.E.A. Mondal conceptualized the study. Kamaal Parvez and M.E.A. Mondal carried out field investigations. Kamaal Parvez drew the diagrams and prepared the first draft of this manuscript. M.E.A. Mondal, Iftikhar Ahmad and Wamiq Mohammed Khan reviewed and edited the manuscript. Kamaal Parvez revised the manuscript.

Funding No funding is available for this research work.

Declarations

Conflict of interest The authors declare that they have no known competing financial interests or personal relationships that could have appeared to influence the work reported in this paper.

References

Acharyya, S.K.: The nature of Mesoproterozoic Central Indian Tectonic Zone with exhumed and reworked older granulites. Gondwana Res. **6**, 197–214 (2003)

Acharyya, S.K., Roy, A.: Tectonothermal history of the central Indian tectonic zone and reactivation of major faults/shear zones. Geol. Soc. India **55**, 239–256 (2000)

Ahmad, I., Latheef, T.P.A., Mondal, M.E.A., Hamidullah, I.S., Parvez, K.: Geochemistry and petrogenesis of the Paleoproterozoic ortho-gneisses and granitoids of the Banded Gneissic Complex, central Rajasthan, NW India: implications for crustal reworking processes. Acta Geochim. **42**, 373–386 (2023). https://doi.org/10.1007/s11631-022-00588-1

Alam, M., Choudhary, A.K., Mouri, H., Ahmad, T.: Geochemical characterization and petrogenesis of mafic granulites from the Central Indian Tectonic Zone (CITZ). Geol. Soc. Lond. Spec. Publ. **449**, 207–229 (2017). https://doi.org/10.1144/SP449.1

Bhattacharya, A., Banerjee, A., Sequeira, N.: The Central Indian Tectonic Zone: a Rodinia supercontinent-forming collisional zone and analogy with the Grenville and Sveconorwegian orogens. Geosphere **19**, 1300–1317 (2023)

Bhowmik, S.K.: The current status of orogenesis in the Central Indian Tectonic Zone: a view from its Southern Margin. Geol. J. **54**, 2912–2934 (2019). https://doi.org/10.1002/gj.3456

Bhowmik, S.K., Pal, T.: Petrotectonic implication of the granulite suite north of the Sausar mobile belt in the overall tectonothermal evolution of the Central Indian mobile belt. Unpubl Prog Rep Geol Surv India (2000). https://doi.org/10.1007/BF02702900

Bhowmik, S.K., Roy, A.: Garnetiferous metabasites from the Sausar Mobile Belt: petrology, P-T path and implications for the tectonothermal evolution of the Central Indian Tectonic Zone. J. Petrol. **44**, 387–420 (2003)

Bhowmik, S.K., Wilde, S.A., Bhandari, A.: Zircon U-Pb/Lu-Hf and monazite chemical dating of the Tirodi biotite gneiss: implication for latest Palaeoproterozoic to Early Mesoproterozoic orogenesis in the Central Indian Tectonic Zone. Geol. J. **46**, 574–596 (2011). https://doi.org/10.1002/gj.1299

Bhowmik, S.K., Wilde, S.A., Bhandari, A., Pal, T., Pant, N.C.: Growth of the Greater Indian Landmass and its assembly in Rodinia: geochronological evidence from the Central Indian Tectonic Zone. Gondwana Res. **22**, 54–72 (2012)

Bhowmik, S.K., Bose, S., Chattopadhyay, A., Karmakar, S., Pant, N.C.: Proterozoic mobile belts-magmatism, metamorphism, geochronology and tectonics in the context of formation of the Greater Indian Landmass. Proc. Indian Natl. Sci. Acad. **90**, 209–240 (2024). https://doi.org/10.1007/s43538-024-00284-z

Bonzi, W.M.-E., Vanderhaeghe, O., Van Lichtervelde, M., Wenmenga, U., André-Mayer, A.-S., Salvi, S., Poujol, M.: Petrogenetic links between rare metal-bearing pegmatites and TTG gneisses in the West African Craton: the Mangodara district of SW Burkina Faso. Precambrian Res. **364**, 106359 (2021)

Bora, S., Kumar, S.: Geochemistry of biotites and host granitoid plutons from the Proterozoic Mahakoshal Belt, central India tectonic zone: implication for nature and tectonic setting of magmatism. Int. Geol. Rev. **57**, 1686–1706 (2015). https://doi.org/10.1080/00206814.2015.1032372

Bora, S., Kumar, S., Yi, K., Kim, N., Lee, T.H.: Geochemistry and U-Pb SHRIMP zircon chronology of granitoids and microgranular enclaves from Jhirgadandi pluton of Mahakoshal Belt, Central India Tectonic Zone. India. J. Asian Earth Sci. **70**, 99–114 (2013)

Bora, S.: Mineralogy Geochemistry and Geochronology of Granitoid Plutons of Dudhi Gneissic Complex Mahakoshal Belt Central India. Doctoral Thesis, Kumaun University, Nainital, India (2015)

Chakrabarty, A., Karmakar, S., Mukherjee, S., Choudhury, S.R., Maiti, P., Sanyal, S., Sengupta, P.: Neoproterozoic reworking of a Mesoproterozoic magmatic arc from the north-eastern part of the Central Indian Tectonic Zone: implication for the growth and disintegration of the Indian shield in the Proterozoic supercontinental cycles. Precambrian Res. **378**, 106758 (2022)

Chattopadhyay, A., Chatterjee, A., Das, K., Sarkar, A.: Neoproterozoic transpression and granite magmatism in the Gavilgarh-Tan Shear Zone, central India: tectonic significance of U-Pb zircon and U-Th-total Pb monazite ages. J. Asian Earth Sci. **147**, 485–501 (2017)

Chattopadhyay, A., Bhowmik, S.K., Roy, A.: Tectonothermal evolution of the Central Indian Tectonic Zone and its implications

for Proterozoic supercontinent assembly: the current status. Episodes J. Int. Geosci. **43**, 132–144 (2020)

Chen, Z.-H., Xing, G.-F.: Geochemical and zircon U-Pb–Hf–O isotopic evidence for a coherent Paleoproterozoic basement beneath the Yangtze Block. South China. Precambrian Res. **279**, 81–90 (2016)

Deshmukh, T., Prabhakar, N., Bhattacharya, A., Madhavan, K.: Late Paleoproterozoic clockwise P-T history in the Mahakoshal Belt, Central Indian Tectonic zone: implications for Columbia supercontinent assembly. Precambrian Res. **298**, 56–78 (2017)

Dwivedi, S.B., Pathak, P., Theunuo, K., Kumar, R.R.: U-Pb SHRIMP zircon dating and geochemistry of metapelites from the Shillong Meghalaya Gneissic Complex, NE India: implications for nature of protolith and tectonic setting. Geosystems Geoenvironment **2**, 100161 (2023)

Giri, R.K., Rao, N.C., Rahaman, W., Kumar, A., Satyanarayanan, M., Krishna, A.K.: Paleoproterozoic calc-alkaline lamprophyres from the Sidhi Gneissic complex, India: implications for plate tectonic evolution of the Central Indian Tectonic Zone. Precambrian Res. **362**, 106316 (2021)

Gupta, S., Kumar, S.: Geochemistry, geochronology, and isotopic studies of Paleoproterozoic magmatic rocks from outer Kumaun Lesser Himalaya, India: implication on petrogenesis and crustal evolution of northern Indian Block. Gondwana Res. **113**, 31–52 (2023)

Huang, C., Chen, B., Sun, K.: A-type granites derived from dehydration melting of calc-alkaline granitoids in East Junggaer (NW China): implications for the origin of aluminous and peralkaline A-types. Lithos **440**, 107043 (2023)

Kaur, P., Chaudhri, N., Raczek, I., Kröner, A., Hofmann, A.W., Okrusch, M.: Zircon ages of late Palaeoproterozoic (ca. 1.72–1.70 Ga) extension-related granitoids in NE Rajasthan, India: regional and tectonic significance. Gondwana Res. **19**, 1040–1053 (2011)

Ketchum, J.W., Barr, S.M., Culshaw, N.G., White, C.E.: U-Pb ages of granitoid rocks in the northwestern Makkovik Province, Labrador: evidence for 175 million years of episodic synorogenic and postorogenic plutonism. Can. J. Earth Sci. **38**, 359–372 (2001). https://doi.org/10.1139/e00-085

Khanna, T.C., Rao, D.S., Bizimis, M., Satyanarayanan, M., Krishna, A.K., Sai, V.S.: 2.1 Ga intraoceanic magmatism in the Central India Tectonic Zone: constraints from the petrogenesis of ferropicrites in the Mahakoshal supracrustal belt. Precambrian Res. **302**, 1–17 (2017)

Kirkland, C.L., Spaggiari, C.V., Pawley, M.J., Wingate, M.T.D., Smithies, R.H., Howard, H.M., Tyler, I.M., Belousova, E.A., Poujol, M.: On the edge: U-Pb, Lu–Hf, and Sm–Nd data suggests reworking of the Yilgarn craton margin during formation of the Albany-Fraser Orogen. Precambrian Res. **187**, 223–247 (2011)

Kröner, A., Rojas-Agramonte, Y., Hegner, E., Hoffmann, K.-H., Wingate, M.T.D.: SHRIMP zircon dating and Nd isotopic systematics of Palaeoproterozoic migmatitic orthogneisses in the Epupa Metamorphic Complex of northwestern Namibia. Precambrian Res. **183**, 50–69 (2010)

Li, G.-Y., Zhou, J.-B., Li, L., Han, J., Song, M.-C.: Paleoproterozoic basement of the Xing'an Block in the eastern Central Asian Orogenic Belt: evidence from the geochemistry and zircon U-Pb geochronology of granitic gneisses. Precambrian Res. **331**, 105372 (2019)

Mandal, B., Sen, M.K., Vijaya Rao, V.: New seismic images of the Central Indian Suture Zone and their tectonic implications. Tectonics **32**, 908–921 (2013). https://doi.org/10.1002/tect.20055

Manya, S., Maboko, M.A.: Generation of Palaeoproterozoic tonalites and associated high-K granites in southwestern Tanzania by partial melting of underplated mafic crust in an intracontinental setting: constraints from geochemical and isotopic data. Lithos **260**, 120–133 (2016)

McDonough, W.F., Sun, S.-S.: The composition of the Earth. Chem. Geol. **120**, 223–253 (1995)

Meert, J.G.: What's in a name? The Columbia (Paleopangaea/Nuna) supercontinent. Gondwana Res. **21**, 987–993 (2012)

Meert, J.G., Pandit, M.K.: The Archaean and Proterozoic history of Peninsular India: tectonic framework for Precambrian sedimentary basins in India. Geol. Soc. Lond. Mem. **43**, 29–54 (2015). https://doi.org/10.1144/M43.3

Mishra, M.K., Alam, M., Kaulina, T.V., Ahmad, T.: Geochemical characterization and zircon U-Pb geochronology of the Tirodi Gneissic Complex, Central Indian Tectonic Zone (CITZ): constraints on petrogenesis, Proterozoic crustal evolution and tectonic setting. Mineral. Petrol. **118**, 159–183 (2024). https://doi.org/10.1007/s00710-024-00853-6

Mohanty, S.P.: Paleoproterozoic thick-skinned tectonics in the Central Indian Tectonic Zone: implications on the tectonic reconstructions of cratonic nuclei. Int. Geol. Rev. **65**, 3028–3064 (2023). https://doi.org/10.1080/00206814.2023.2172620

Nair, K.K.K.: Stratigraphy, structure and geochemistry of the Mahakoshal greenstone belt. Mem. Geol. Soc. India **31**, 403–432 (1995)

Narain, A., Thambi, P.I. 1977: Geology and structure of Khaddi-Gajrahi area, Gopad-Banas Tehsil, Sidhi districts, MP Geol. Surv India Unpubld Rep. FS 78

Narayanaswamy, S., Chakraborty, S.C., Vemban, N.A., Shukla, K.D., Subramanyam, M.R., Venkatesh, V., Rao, G.V., Anandalwar, M.A., Nagarajaiah, R.A.: The geology and manganese ore deposits of the manganese belt in Madhya Pradesh and adjoining parts of Maharashtra. Bull. Geol. Surv. India Ser. A **22**, 69 (1963)

Okonkwo, C.T., Ganev, V.Y.: U-Pb Geochronology of the Jebba granitic gneiss and its implications for the paleoproterozoic evolution of Jebba area, southwestern Nigeria. Int. J. Geosci. **3**, 1065–1073 (2012)

Parvez, K., Mondal, M.E.A., Ahmad, I., Rahaman, W., Shukla, A.D., Khan, W.M.: mineralogical, geochemical and nd isotopic study of the meta-clastic rocks of the paleoproterozoic Mahakoshal Basin, Central Indian Tectonic Zone: implications for provenance characterization, paleoweathering conditions and tectonic setting. Geochem. Int. **62**, 1378–1404 (2024a). https://doi.org/10.1134/S0016702924700472

Parvez, K., Mondal, M.E.A., Amal Dev, J., Ahmad, I., Khan, W.M., Tomson, J.K.: Geochemistry and geochronology of 1.7-1.8 Ga peraluminous A-type granites and granite-gneiss from the Mahakoshal Basin, Central Indian Tectonic Zone (CITZ): implications for an accretionary orogen for the evolution of CITZ. Int. Geol. Rev. **67**, 675–693 (2024b). https://doi.org/10.1080/00206814.2024.2400694

Petford, N., Kerr, R.C., Lister, J.R.: Dike transport of granitoid magmas. Geology **21**, 845–848 (1993)

Petford, N., Lister, J.R., Kerr, R.C.: The ascent of felsic magmas in dykes. Lithos **32**, 161–168 (1994)

Petford, N., Cruden, A.R., McCaffrey, K.J.W., Vigneresse, J.-L.: Granite magma formation, transport and emplacement in the Earth's crust. Nature **408**, 669–673 (2000)

Radhakrishna, B.P., Naqvi, S.M.: Precambrian Continental Crust of India and its evolution. J. Geol. **94**, 145–166 (1986). https://doi.org/10.1086/629020

Raju, S., Rastogi, S.P.: Atlas of granites of southern Uttar Pradesh, India. In: Catalogue Series, p. 141. Geological Survey of India, Guindy (2001)

Ramakrishnan, M., Vaidyanadhan, R.: Geology of India. Geological Society of India Bangalore, Bangalore (2008)

Rogers, J.J., Santosh, M.: Configuration of Columbia, a Mesoproterozoic supercontinent. Gondwana Res. **5**, 5–22 (2002)

Rogers, J.J., Santosh, M.: Supercontinents in earth history. Gondwana Res. **6**, 357–368 (2003)

Roy, A., Prasad, M.H.: Tectonothermal events in Central Indian Tectonic Zone (CITZ) and its implications in Rodinian crustal assembly. J. Asian Earth Sci. **22**, 115–129 (2003)

Sarkar, S.N., Trivedi, J.R., Gopalan, K.: Rb-Sr whole-rock and mineral isochron ages of the Tirodi gneiss, Sausar group, Rhandara district. Maharashtra. J. Geol. Soc. India **27**, 30–37 (1986)

Sarkar, A., Bodas, M.S., Kundu, H.K., Mamgain, V.D., Shanker, R.: Geochronology and geochemistry of mesoproterozoic intrusive plutonites from the eastern segments of the Mahakoshal greenstone belts, Central India. In: Seminar on Precambrian Crust in Eastern and Central India, pp. 82–85. IGCP, Bhubneshwar (1998)

Sharma, A., Das, K., Chakraborty, P.P., Shiraishi, F., Kayama, M.: U-Pb zircon geochronology of a pyroclastic rock from the Parsoi Formation, Mahakoshal Group: implications towards age and tectonics of the Basin in Central Indian Tectonic Zone. Geol. J. **57**, 4122–4138 (2022). https://doi.org/10.1002/gj.4533

Sheppard, S., Occhipinti, S.A., Tyler, I.M.: A 2005–1970 Ma Andean-type batholith in the southern Gascoyne complex, Western Australia. Precambrian Res. **128**, 257–277 (2004)

Shukla, M., Verma, S.K., Malviya, V.P., Oliveira, E.P., Mishra, S., Umrao, R.K., Prakash, S., Torres, E.E.M.: Crustal reworking during the transition of tectonic regime in the Paleoproterozoic Era: constraints from geochemistry, Sm-Nd isotope and U-Pb geochronology of granitic gneisses, Dudhi Granitoid Complex, Mahakoshal belt, Central Indian Tectonic Zone (CITZ). India. Precambrian Res. **417**, 107660 (2025)

Stein, H.J., Hannah, J.L., Zimmerman, A., Markey, R.J., Sarkar, S.C., Pal, A.B.: A 2.5 Ga porphyry Cu–Mo–Au deposit at Malanjkhand, central India: implications for Late Archean continental assembly. Precambrian Res. **134**, 189–226 (2004)

Wang, L.-X., Ma, C.-Q., Zhang, C., Zhu, Y.-X., Marks, M.A.: Halogen geochemistry of I-and A-type granites from Jiuhuashan region (South China): insights into the elevated fluorine in A-type granite. Chem. Geol. **478**, 164–182 (2018)

Wang, J., Yang, C., Wyman, D.A., Song, H., Du, L.: Petrogenesis and tectonic implications of the 2.1–2.0 Ga granitoids in Fuping Complex, North China Craton: constraints from petrology, geochemistry and zircon U-Pb-Hf isotopes. Precambrian Res. **339**, 105611 (2020a)

Wang, Y., Yang, Y.-Z., Siebel, W., Zhang, H., Zhang, Y.-S., Chen, F.: Geochemistry and tectonic significance of late Paleoproterozoic A-type granites along the southern margin of the North China Craton. Sci. Rep. **10**, 86 (2020b)

Wani, H., Mondal, M.E.A.: Geochemical evidence for the Paleoproterozoic arc–back arc basin association and its importance in understanding the evolution of the Central Indian Tectonic Zone. Tectonophysics **690**, 318–335 (2016)

Wani, H., Mondal, M.E.A., Ahmad, I.: Geochemistry of metasedimentary rocks of the Sonakhan and Mahakoshal greenstone belts, Central India: implications for paleoweathering, paleogeography and mechanisms of greenstone belt development. Acta Geochim. **41**, 64–83 (2022). https://doi.org/10.1007/s11631-021-00496-w

Yadav, B.S., Ahmad, T., Kaulina, T., Bayanova, T., Bhutani, R.: Origin of post-collisional A-type granites in the Mahakoshal Supracrustal Belt, Central Indian Tectonic Zone, India: Zircon U-Pb ages and geochemical evidences. J. Asian Earth Sci. **191**, 104247 (2020)

Yadav, B.S., Ahmad, T., Kaulina, T., Bayanova, T. 2015: Geochemistry, U-Pb zircon chronology and Sm-Nd characteristics of granitoids from Central Indian Tectonic Zone (CITZ). Goldschmidt Abstr. Prague Czech Repub. 3483.

Yedekar, D.B., Jain, S.C., Nair, K.K.K., Dutta, Kk.: The central Indian collision suture. Visesa Prakasana-Bharatiya Bhuvaijñanika Sarveksana **28**, 1–43 (1990)

Zhao, G., Sun, M., Wilde, S.A., Li, S.: Assembly, accretion and breakup of the Paleo-Mesoproterozoic Columbia Supercontinent: records in the North China Craton. Gondwana Res. **6**, 417–434 (2003)

Zhao, J., Zhang, C., Liu, X., Gan, J.: Middle Paleoproterozoic tectonic evolution of the Trans-North China Orogen, North China Craton: constraint from the intermediate-acid magmatism in the Lüliang area. Lithos **378**, 105804 (2020)

Publisher's Note Springer Nature remains neutral with regard to jurisdictional claims in published maps and institutional affiliations.

Springer Nature or its licensor (e.g. a society or other partner) holds exclusive rights to this article under a publishing agreement with the author(s) or other rightsholder(s); author self-archiving of the accepted manuscript version of this article is solely governed by the terms of such publishing agreement and applicable law.